Carbohydrate Polymers 97 (2013) 327–334

Contents lists available at SciVerse ScienceDirect

Carbohydrate Polymers

journal homepage: www.elsevier.com/locate/carbpol

Highly luminescent chitosan-L-cysteine functionalized CdTe quantum dots film: Synthesis and characterization

Hridyesh Kumar[a], Rohit Srivastava[a,b], P.K. Dutta[a,*]

[a] Department of Chemistry, Motilal Nehru National Institute of Technology, Allahabad 211004, India
[b] Department of Applied Chemistry, Birla Institute of Technology, Deoghar Campus, 814142, India

ARTICLE INFO

Article history:
Received 4 January 2013
Received in revised form 11 April 2013
Accepted 13 April 2013
Available online 15 May 2013

Keywords:
Luminescence
Quantum dots
L-Cysteine
Chitosan
Antibacterial activity

ABSTRACT

The present work describes synthesis of water soluble L-cysteine-functionalized CdTe quantum dots (QDs) with size tunable emission at different time intervals for chitosan based film. The characterization of the synthesized CdTe QDs–chitosan film was made by Fourier transform infrared (FTIR) spectroscopy, X-ray diffraction (XRD), differential scanning calorimetry (DSC), thermo gravimetric analysis (TGA) and scanning electron microscope (SEM). The optical property of CdTe QDs–chitosan film was determined by UV–vis and photo-luminescence (PL) spectroscopy whereas their antibacterial activity was screened for Gram positive (*Staphylococcus aureus*) as well as Gram negative (*Pseudomonas aurigionasa* and *Escherichia coli*) bacteria by disc diffusion method. The loss of tunable light emission effect of QDs as well as the positive result of antibacterial study reveals that the synthesized QDs based chitosan film is a promising candidate for wide range of biomedical applications.

1. Introduction

Nano-sized luminescent semiconductor crystal from group II–VI and III–V elements is commonly termed as quantum dots (QDs), such as, CdSe (Qu, Peng, & Peng, 2001), CdTe (Talapin et al., 2001), CdS (Murray, Norris, & Bawendi, 1993) and ZnSe (Chen et al., 2004). Their unique size/composition, tunable narrow emission and broad absorption spectra (Zhong, Han, Dong, White, & Knoll, 2003) exhibit a vast range of applications, such as light-emitting devices, non-linear optical devices, solar cells and fluorescent bio-labels (Bailey & Nie, 2003; Bruchez, Moronne, Gin, Weiss, & Alivisatos, 1998; Chen et al., 2004; Jaiswal, Mattoussi, Mauro, & Simon, 2003; Mamedov, Belov, Giersig, Mamedova, & Kotov, 2001). Compared with organic fluorescent dye, QDs exhibit more robust fluorescence intensity, greater photostability, broader excitation wavelength range and narrow emission spectrum (Medintz, Uyeda, Goldman, & Mattoussi, 2005). The broad absorption and narrow emission spectra of the QDs make them excellent donors in fluorescence resonance energy transfer (FRET) based sensors. To date, most of the QDs are prepared in the organic phase and their surfaces are functionalized with various capping agents like L-cysteine, dihydrolipoic acid (DHLA), glutathione (GTH) (Qian, Dong, Weng, & Ren, 2006), folic acid and mercaptoundecanoic acid (Jiang, Mardyani, Fischer, & Chan, 2006). Trend is changing now, an aqueous synthesis of QDs display great improvement due to ease in synthesis, low reaction temperature, low toxicity chemical and more notably water soluble QDs has potential widespread application in the field of biomedical (Li, Jing, Qiao, & Gao, 2011). The biomedical and clinical applications of QDs are limited due to their poor biocompatibility and instability in physiological environment. Several approaches have been developed to overcome these problems, out of them; one of the most successful approaches is to coat QDs with biocompatible polymers.

Natural as well as synthetic both type of polymers are used in biomedical field. Nowadays biopolymers such as chitosan, hyaluronan and chondroitin sulfate are mostly used to deliver oligonucleotides, DNA, proteins and drugs (Muzzarelli, Boudrant, et al., 2012; Muzzarelli, Greco, et al., 2012). Among all the natural polymers, chitosan has increased much attention in recent years for biomedical applications (Jayasree, Sasidharan, Koyakutty, Nair, & Menon, 2011; Ravi Kumar, Muzzarelli, Muzzarelli, Sashiwa, & Domb, 2004; Sanpui, Pandey, Chattopadhyay, & Ghosh, 2010; Yuan, Hein, & Misra, 2010). Besides chitosan, its other derivatives like N-(O-carboxybenzyl) chitosan, N-carboxymethyl chitosan and dithiocarbamate chitosan have also been investigated and used in biomedical application (Muzzarelli & Tanfani, 1982). Chitosan is the second most abundant biopolymer in nature after cellulose. It is a linear polysaccharide consisting of β-(1, 4) linked D-glucosamine residues and N-acetyl-glucosamine group which is obtained from chitin by deacetylation (Muzzarelli, Boudrant, et al., 2012; Muzzarelli, Greco, et al., 2012). Chitosan has some

* Corresponding author. Tel.: +91 532 2271272; fax: +91 532 2545341.
E-mail address: pkd_437@yahoo.com (P.K. Dutta).

0144-8617/$ – see front matter © 2013 Elsevier Ltd. All rights reserved.
http://dx.doi.org/10.1016/j.carbpol.2013.04.056

unique properties including biocompatibility, biodegradability, hydrophilicity, non-toxicity, non-antigenicity, bio-adherence and cell affinity. It is the only positively charged naturally occurring polysaccharide which strongly interacts with negatively charged entities. Besides, owing to its low cost, large-scale availability and antimicrobial activity (Eugene & Lee, 2003) it possesses special properties, such as suitable for blood-brain barrier (Aktaş et al., 2005), haemostatic agent, and fat attractor (Chung & Chen, 2008). This unique property is very advantageous in several biomedical applications; particularly on chitosan based functional nanomaterials (Dutta, Srivastava & Dutta, in press).

Compared with other colloidal carriers, polymeric nanoparticles present a higher stability when in contact with biological fluids, and their polymeric nature enables controlled and sustained drug release (Maria, Didier, Patrick, & d'Angelo, 1997). Chitosan is also widely used in biomedical field as a carrier for drugs or other biomaterials (Liong et al., 2008) and its chelating ability make it a suitable matrix for functionalized QDs. Chitosan as a cationic polyelectrolyte enhances the cellular binding and internalization of QDs for *ex vivo* cell labelling. Several works based on QDs–chitosan conjugate system such as water-soluble chitosan–quantum dot hybrid nanospheres (Lin et al., 2011), Mannosylated chitosan-zinc sulphide nanocrystals (Jessirie, Hilton, & Amandav, 2009), carboxymethyl chitosan coated CdTe/CdS quantum dots (He, Zhu, & Zhou, 2012), functionalized chitosan/quantum dot nano-hybrids (Mansur, Mansur, Curti, & Almeida, 2013), explain importance of chitosan–quantum dot system in biomedical fields with specific focus on nanomedicine, biosorbing, biosensing and bioimaging application. Considering the advantageous properties mentioned above of both QDs, chitosan and chitosan–quantum dot systems, we have investigated a facile approach to synthesize L-cysteine-functionalized CdTe QD-chitosan nanocomposite film through amide bond formation. The loss of tunable light emission effect as well as the enhanced antibacterial properties of the QDs–chitosan nanocomposite film will help to present a promising material for biomedical applications.

2. Experimental

2.1. Materials

Chitosan powder was obtained from Aldrich (USA) with average molecular weight about < 5000 g/mole (Mw) and degree of deacetylation of 85%. Cadmium chloride, sodium borohydride, tri-sodium citrate dihydrate, L-cysteine and sodium tellurite were purchased from Aldrich (USA). For antibacterial activity, Muller Hinton Agar (MHA) was purchased from Himedia Pvt. Ltd. Mumbai (India).

2.2. Characterization

Fourier transform infrared spectroscopy (FTIR) measurements were recorded on Perkin Elmer RX1 spectrophotometer,

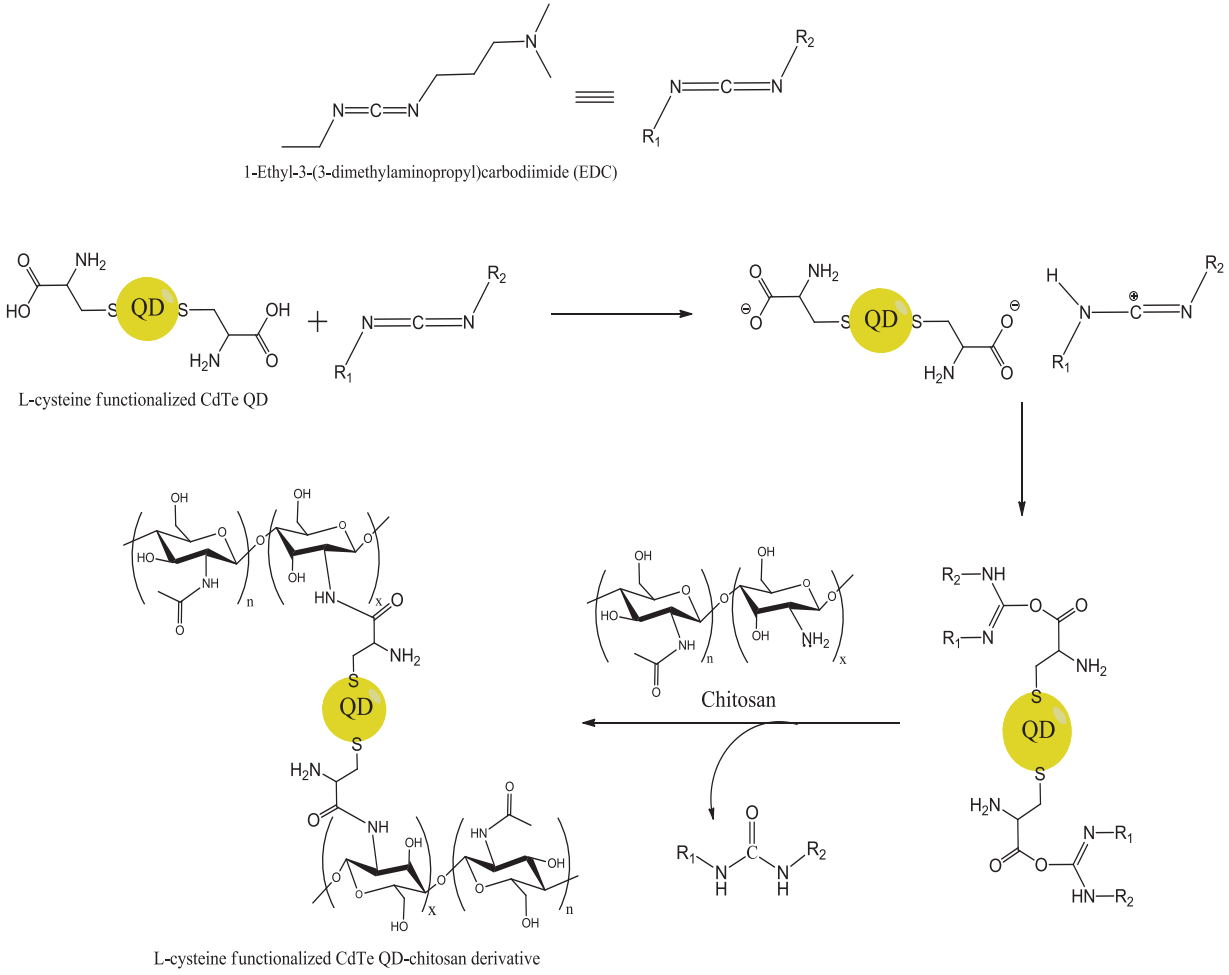

Scheme 1. Preparation of L-cysteine-functionalized-CdTe quantum dots (QDs)–chitosan derivative containing amide linkage.

differential scanning calorimetry (DSC) and thermo gravimetric analysis (TGA) was performed with Perkin Elmer Pyris 6 at a heating rate of 10 °C under nitrogen atmosphere. The Morphology was studied by using scanning electron microscope (SEM) with JEOL JSM840 at 15 kV and transmission electron microscope (TEM) with Morgani (FEI) Netherland 268 D, operated on accelerating voltage of 60–80 kV at 50 nm resolutions.

UV–vis spectra were recorded on Schimadzu UV-2450 UV-vis spectrophotometer using 1.0 cm quartz cell at ambient temperature. The PL spectra were recorded on Perkin Elmer LS55 fluorescence spectrometer and XRD measurements were performed with XPERT-PRO (PW 3050/60) using Cu Kα radiation (γ = 1.54060 Å) operated at 30 kV and 30 MA.

2.3. Antibacterial test

The antibacterial test of the prepared CdTe QDs–chitosan film and its components were performed according to the recommendations of National Committee for Clinical Laboratory Standards (NCCLS) (Clark, Jacobs, & Appelbaum, 1998) by disc diffusion methods using Gram positive (*Staphylococcus aureus* MTCC No. 3160) as well as Gram negative (*Pseudomonas aurigionasa* MTCC No. 1688 and *Escherichia coli* MTCC No. 1303) bacteria. These microorganisms were obtained from Institute of Microbial Technology, Chandigarh, India. The solidified LB agar plates were swabbed with 100 μl of *E. coli* (gram negative) and solidified NB agar plates were swabbed with 100 μl of *S. aureus* (gram positive), *P. aurigionasa* (gram negative) bacteria. Before starting antibacterial assessment, all the glass wares were sterilized by autoclaving them for 30 min at 120 °C under 15 lbs. pressure. The wells were prepared on the LB and NB agar plates with the help of a cork borer (6 mm diameter) For disc diffusion method, the CdTe QDs–chitosan film was cut into a disc shape with 6 mm diameter and placed in cultured agar plates. All these processes were done in a laminar air flow chamber. These plates were incubated for 24 h at 37 °C. After 24 h the zone of inhibition was measured with the help of ruler. If there is no clear zone surrounding, we assumed that there is no inhibitory zone and furthermore, the diameter was valued as zero.

2.4. Synthesis

We have synthesized L-cysteine functionalized CdTe QDs–chitosan film in two steps which is described as follows:

2.4.1. Synthesis of L-cysteine functionalized CdTe QDs

L-Cysteine functionalized CdTe QDs with different emission capability were synthesized with some modification for better results (Bao, Wang, & Dong, 2006). In typical experiment, 4 ml of 0.04 mol L^{-1} cadmium chloride ($CdCl_2$) solution was diluted with 50 ml double distilled water in a round bottom flask. Then 100 mg tri-sodium citrate dihydrate, 4 ml of 0.01 mol L^{-1} sodium tellurite (Na_2TeO_3), 50 mg L-cysteine and 50 mg sodium borohydride ($NaBH_4$) was added with continuous stirring. The flask was attached to a condenser and refluxed at 100 °C under open air conditions. Tri sodium citrate dihydrate was added to avoid the deposition of cadmium tellurite ($CdTeO_3$). At different time interval, CdTe colloidal solution was taken out from reaction mixture to check tunability in emission wavelength (from green to dark orange) under short UV light at 256 nm which was observed to increase in size of CdTe in colloidal solution (Fig. 1a). During entire synthesis of L-cysteine functionalized CdTe QDs, following chemical reactions takes place.

$$4TeO_3^{2-} + 3BH_4^- \rightarrow 4Te^{2-} + 4BO_2^- + 6H_2O$$

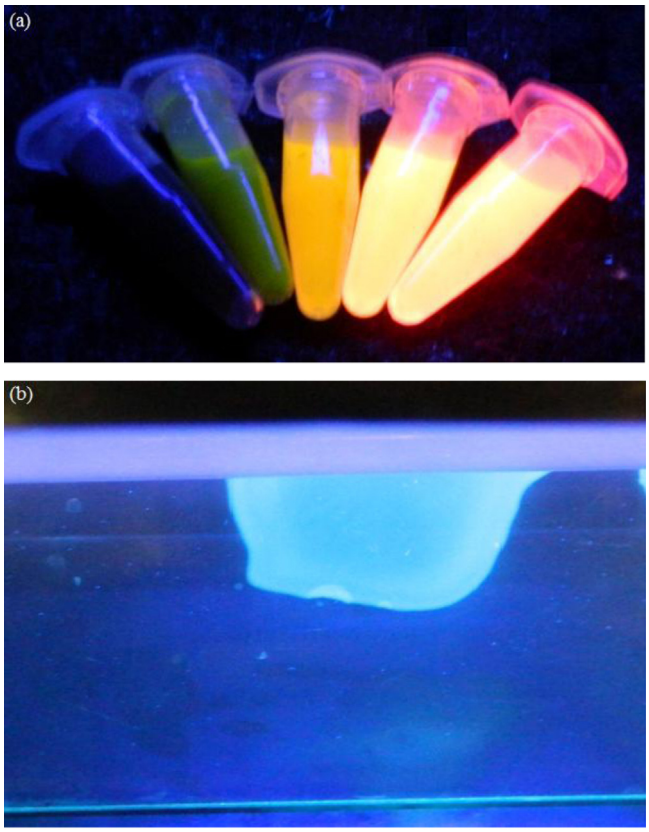

Fig. 1. (a) Tunability in emission of aqueous CdTe under short wave UV in samples taken after 30 min (black), 45 min (green), 75 min (yellow), 120 min (light orange) and 180 min (dark orange). (b) CdTe QDs–chitosan film under shortwave UV.

$$CdCys + Te^{2-} \rightarrow CdTe + Cys, \quad Cys = \text{cysteine}$$

2.4.2. Synthesis of L-cysteine functionalized CdTe QDs–chitosan film

For the synthesis of CdTe QDs–chitosan film, in 1% chitosan solution, calculated amount of CdTe QDs with 1-ethyl-3-(3-dimethylaminopropyl) carbodiimide (EDC) was added. The complex solution was stirred overnight at room temperature and was poured onto a ceramic plate. The plate was placed in vacuum oven (Yamato ADP200) at 50 °C for 24 h to get a dried and highly luminescent film (Fig. 1b). All the reaction steps have been shown in Scheme 1.

2.5. Swelling study

Six pieces of CdTe QDs–chitosan film (13 mg each) were cut in a cubic shape and equilibrated in six different small beakers containing 15 ml of water with pH 7.4 and beakers were placed in an incubator at 37 °C temperature. The water uptake by the films was measured by electronic balance at every 40 min up-to the equilibrium. The swelling ratio of the CdTe QDs–chitosan film was calculated by following formula

$$\text{Swelling ratio (SR)} = \left[\frac{(W_s - W_o)}{W_o}\right] \times 100$$

where W_o is an initial weight of dry film and W_s is the swollen weight of film at equilibrium.

3. Result and discussion

3.1. Characterization

3.1.1. UV–vis spectroscopy

Chitosan itself is a transparent in the UV and visible region, so its conformation is hard to characterize by UV spectroscopic method. We can overcome this natural handicap by borrowing chromophores from extrinsic molecule. The UV–vis spectra of CdTe QDs and CdTe QDs–chitosan film shows absorption band at 400 nm and 350 nm respectively.

3.1.2. Photoluminescence (PL) spectroscopy

The PL spectra of chitosan, L-cysteine functionalized CdTe QDs and CdTe QDs–chitosan films are shown in Fig. 2. A PL spectrum of chitosan (Fig. 2a) shows a broad band emission between 440 and 515 nm with 164 PL intensity followed by 380 nm excitation whereas PL spectra of L-cysteine functionalized CdTe QDs (Fig. 2b) shows emission wavelength at 525 nm when exciting it by 450 nm. The probable reason for this emission may be due to the presence of acid moiety of L-cysteine. PL spectra of CdTe QDs–chitosan film (Fig. 2c) shows emission wavelength at 514 nm while exciting it by 450 nm. The probable reason for this emission may be due to the presence of chitosan component as a

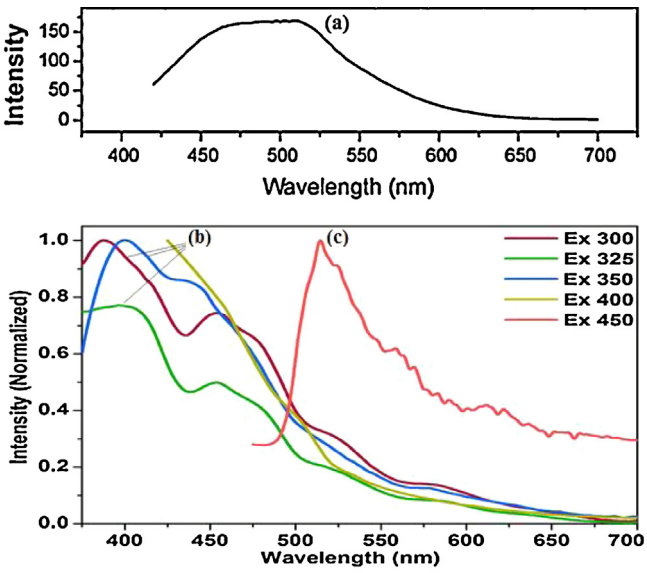

Fig. 2. PL graph of chitosan (a), CdTe QDs (b) and CdTe QDs–chitosan film (c).

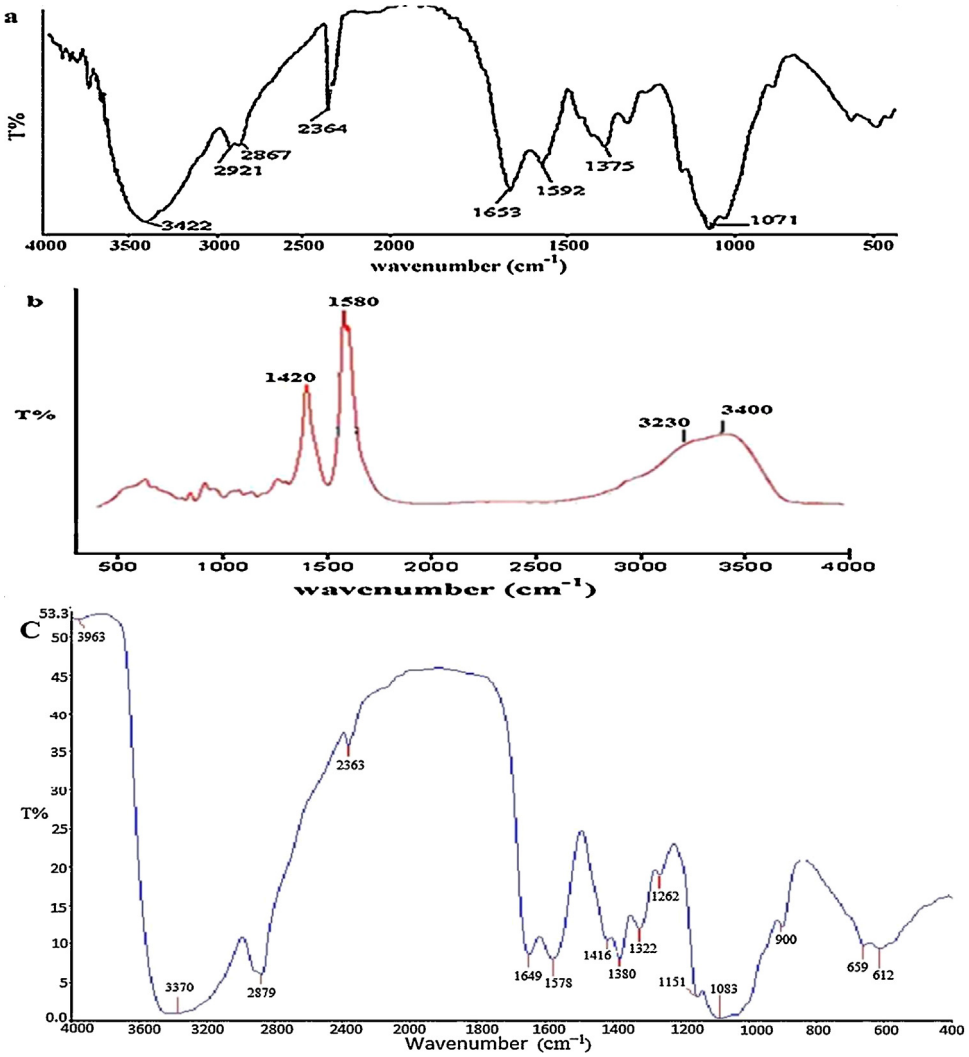

Fig. 3. IR spectra of chitosan (a), CdTe QDs (b) and CdTe QDs–chitosan film (c).

result of big size molecule and thus it shows loss of tunability of QDs in the CdTe QDs–chitosan film. It was observed that at the same excitation wavelength (450 nm) the CdTe QDs shows 525 nm emission wavelengths whereas CdTe QDs–chitosan film shows 514 nm emission wavelengths. The comparative blue shift in emission of CdTe QDs–chitosan film is due to its electrostatic conjugation with L-cysteine functionalized CdTe QDs. A blue shift is also observed in the absorption spectra that validate the finding obtained by PL. The side chain containing electron withdrawing group decreases the emission intensity while electron donating group increases it (Kumar & Dutta, 2008; Singh & Dutta, 2009).

The tunable light emission result of QDs–chitosan film is the positive indication of biomedical application in terms of tracking the cells and intracellular processes through biosignalling.

3.1.3. Fourier transform infrared spectroscopy (FTIR)

The infrared spectra of chitosan, L-cysteine functionalized CdTe QDs and CdTe QDs–chitosan film are shown in Fig. 3. For chitosan spectrum (Fig. 3a), the absorption band observed at 3422 cm^{-1} (O—H stretch overlapped with N—H stretch), 2921 and 2867 cm^{-1} (C—H stretch), 2364 cm^{-1} (C—N asymmetric band stretching), 1653 cm^{-1} (amide II band, C—O stretch of acetyl group), 1592 cm^{-1} (amide II band, N—H stretch), 1375 cm^{-1} (asymmetric C—H bending of CH_2 group) and 1071 cm^{-1} (skeletal vibration involving the bridge C—O stretch) of glucosamine residue (Singh, Kumar, & Dutta, 2009). In the IR spectra of L-cysteine functionalized CdTe QDs (Fig. 3b) the absorption band appears at 2550 and 945 cm^{-1} due to the S—H stretching and bending modes because of the cleavage of the S—H bond and the formation of a new S—Cd bond between cysteine and CdTe nanoparticles. The appearance of broad band at 3396 and 3210 cm^{-1} could be assigned to the asymmetric and symmetric stretching of $-NH_2$. Peaks of ν(C—H) are in the region of 2969–2850 cm^{-1}. It can be observed that there is a shift of the stretching vibration of the carboxyl group in cysteine from 1604 to 1574 cm^{-1}, implying that the carboxyl group of cysteine turned into its anion and led to intense symmetric vibration of the carboxyl anion at 1410 cm^{-1} (Demarger-Andre & Domard, 1994). The IR spectrum of CdTe QDs–chitosan film (Fig. 3c) exhibit an absorption around 1650 cm^{-1} (C=O stretch, amide I) and 1578 cm^{-1} (N—H bend, amide II) which represents the amide I and amide II bands respectively. There are bands at 1414 cm^{-1}, 1380 cm^{-1} and 1322 cm^{-1}, in addition to the usual C—H aliphatic band at 2879 cm^{-1}. The O—H and NH_2 overlapping broad band are found around 3310–3460 cm^{-1}.

3.1.4. Thermal analysis

The TGA graph of chitosan and L-cysteine functionalized CdTe QDs–chitosan film are shown in Fig. 4. In TGA graph of chitosan (Fig. 4a) there is a weight loss of 12% in the temperature range 140–200 °C due to the decomposition of polymer and the weight loss of 38% in the temperature range 200–310 °C is due to the dehydration of saccharide rings. The TGA graph of L-cysteine functionalized QDs–chitosan film has been shown in Fig. 4b. The weight loss of 4% in the temperature range 48–114 °C is due to the residual water present in the sample, weight loss of 9% in the temperature range 196–255 °C is due to the degradation of chitosan chain and weight loss of 15% in the temperature range 332–522 °C is due to the decomposition of CdTe QDs–chitosan film. It is found that the weight loss of CdTe QDs–chitosan film is quite small because of removal of absorbed physical and chemical water.

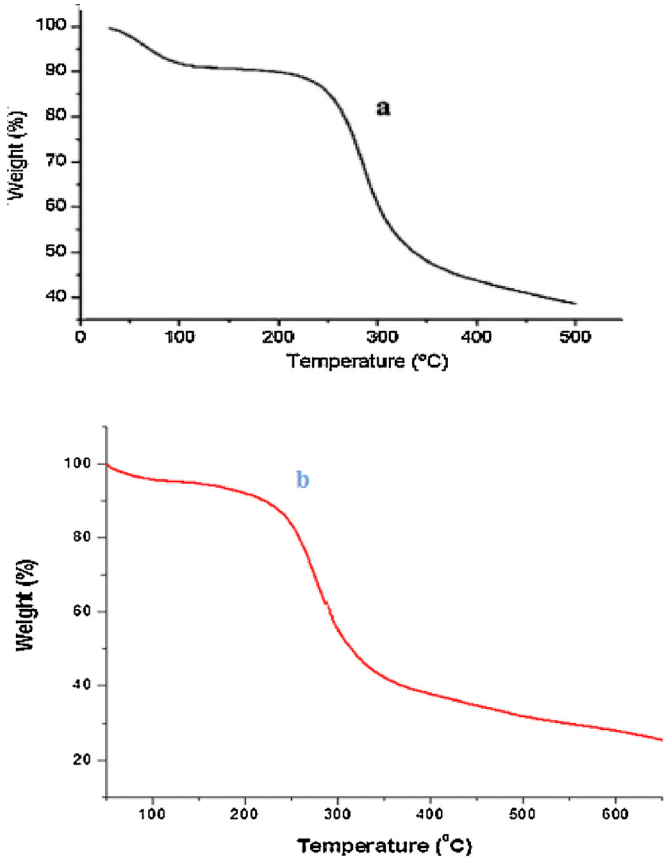

Fig. 4. TGA graph of chitosan (a), and CdTe QDs–chitosan film (b).

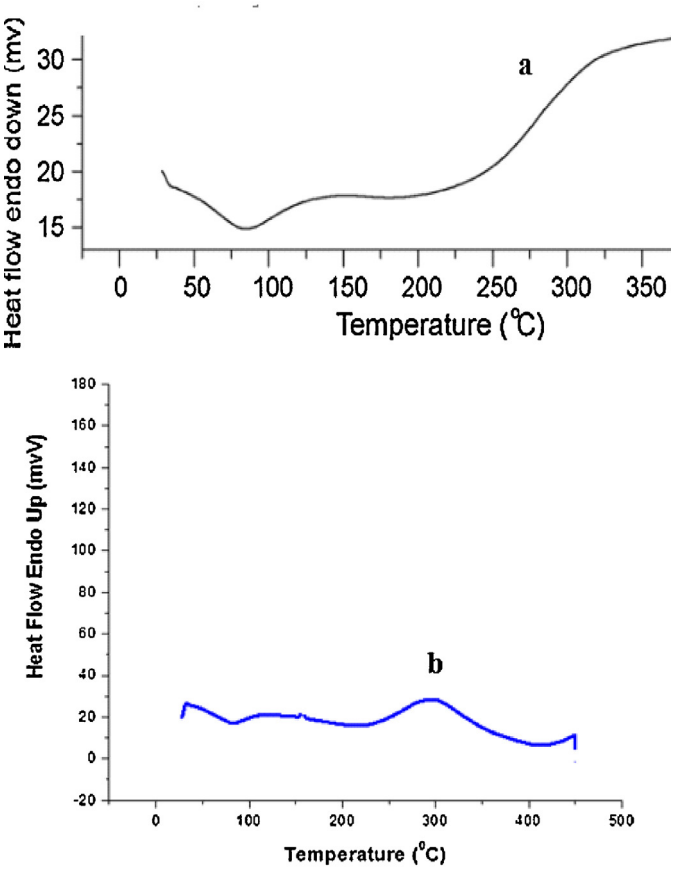

Fig. 5. DSC graph of chitosan (a) and CdTe QDs–chitosan film (b).

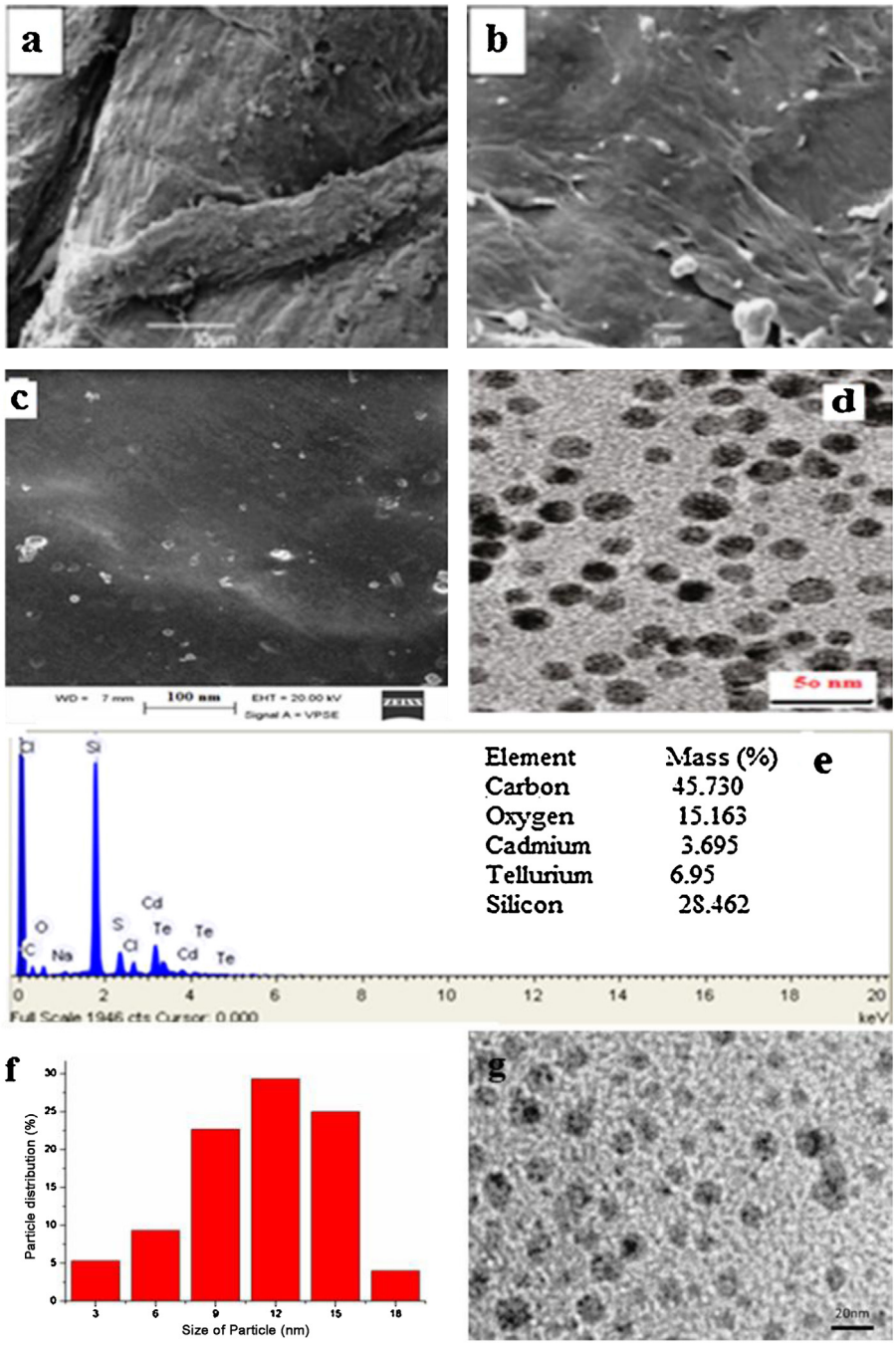

Fig. 6. SEM images of chitosan (a and b), CdTe QDs–chitosan film (c), TEM image of CdTe QDs and EDX graph of CdTe QDs (e), histogram of CdTe QDs (f) and TEM image of CdTe QDs–chitosan film (g).

There was no significant variation in weight from 522 °C to 700 °C, implying the presence of only CdTe QDs within the temperature range.

3.1.5. Differential scanning calorimetry

The DSC thermograms of chitosan and L-cysteine functionalized CdTe QDs–chitosan film are shown in Fig. 5. The thermal spectrum of chitosan (Fig. 5a) shows two broad endothermic peaks at 92.3 and 212.5 °C. The former peak may be due to the water present in chitosan while the latter may be attributed to the decomposition of chitosan whereas DSC thermogram of L-cysteine functionalized CdTe QDs–chitosan film (Fig. 5b) shows three small peaks at 31, 153 and 294 °C corresponding to the structural arrangement and its degree of substitutional changes. The results indicate that the structure of chitosan chains have been changed due to the introduction of acid moieties and the reduced ability of crystallization.

3.1.6. Morphology study

The SEM images (Fig. 6a and b) of the chitosan contain a non-porous, smooth membranous phase consisting of dome shape orifices, microfibrils and crystallites. It also exhibited flat lamellar phases on which a large number of protruding microfibrils are evident. Fig. 6c shows a typical SEM image of CdTe QDs–chitosan film. It is observed that the CdTe QDs–chitosan film took the spherical shape. A TEM micrograph of the chemically synthesized CdTe QDs is shown in Fig. 6d. The TEM micrograph suggests polydisperse

Table 1
Zone of Inhibition CdTe QDs–chitosan film and its components against different microorganisms.

Sample code	Zone of inhibition in mm for the bacteria		
	Pseudomonas aeruginosa	*Staphylococus aureus*	*Escherichia coli*
CH	15.0	16.1	18.2
CdTe QD (bare)	17.1	18.0	20.2
CdTe QDs–chitosan film	20.4	22.1	24.0

nature of CdTe QDs. By using histogram (Fig. 6f), we have found the average particle size is about 12 nm with a wide range dispersion of 3–18 nm. The TEM micrograph of CdTe QDs–chitosan composite showing uniformly dispersed CdTe QDs in chitosan matrix retaining their size distribution stuck by agglomeration (Fig. 6g).

3.2. Swelling property

Swelling is one of the most important properties of chitosan derivative film for biomedical applications. Swelling study analysis of CdTe QDs–chitosan film shows maximum swelling ratio (460%) at 217 min. After maximum swelling, the film attains equilibrium i.e., weight of the film neither increased nor decreased. This stability after maximum swelling is due to strong bond formation between amine group of chitosan and carboxyl group of CdTe QDs which hamper protonation of amino group of chitosan (Li, Ramay, Hauch, Xiao, & Zhang, 2005).

3.3. Antibacterial study

Bacteria rapidly evolve mechanism to become resistant to antibiotics. Therefore identifying an effective antibiotic or antibacterial agent and administering it at concentrations that will successful prevent bacterial growth is critical for healthcare decision making and is vital for the battle against multidrug-resistant bacteria (Nath, Kaittanis, Tinkham, & Perez, 2008). So the minimum inhibition concentration (MIC) determination was carried out to find the concentrations of antibiotic required for microbial inhibition. Chitosan based antibacterial films are of great importance due to their excellent biomedical applications (Liu, Xue, & Ding, 2009; Srivastava, Tiwari, & Dutta, 2011). Although a lot of synthetic polymer based nanocomposites have been employed as surgical and wound dressing materials but they often regenerates skin irritations due to leaching of harmful chemicals and causes side effects. Therefore, generation of antimicrobial films using renewable natural sources and biopolymers would be better options.

In our present investigation, we have screened our novel CdTe QDs–chitosan film for their antibacterial activity and it was found that it has greater activity in compression to that of its basic components, i.e., chitosan (CH) and L-cysteine functionalized CdTe QDs. The MIC for nanocomposite film was observed 90 μg/ml and for water soluble L-CdTe QDs 50 μg/ml for both microorganism. The zone of inhibition of prepared CdTe QDs–chitosan film and its components have been shown in Table 1.

From Table 1 we have found that L-cysteine functionalized CdTe QDs–chitosan film exhibit significantly higher antibacterial activity and higher zone of inhibition than its components at their respective concentration for both microorganisms.

It has been documented that CdTe QDs show antibacterial activity by producing very reactive singlet oxygen species (Rameshkumar et al., 2013). CdTe QDs could not enter into bacteria through its membrane due to bigger size. Quantum dot requires a bioconjugate which damage membrane and facilitate QDs entry in to inner environment (Luo, Wu, Zhang, Li, & Ding, 2011). Chitosan, a cationic polymer, itself show antibacterial activity by interacting with negatively charged bacterial membrane which leads to membrane disruption and leakage of intracellular element (Rabea, Badawy, Stevens, Smagghe, & Steurbaut, 2003). The chitosan facilitate inclusion of CdTe QDs into intracellular environment infuses cell death caused by singlet oxygen species. Therefore, synchronous effect of novel CdTe QDs–chitosan film enables better antibacterial activity relative to its pristine component.

4. Conclusion

Our present study demonstrates successful preparation of L-cysteine functionalized CdTe QDs–chitosan film in a facile two step process. From the PL and UV–vis spectra it is evident that the film has blue shift compared to pristine chitosan which confirms the loss of tunability of QDs during formation of QDs–chitosan derivative indicating that the film would be useful for tracking the cells and intracellular processes through bio-signalling. The result of antibacterial study revealed that the prepared film is more effective in comparison to all of its individual components at their respective concentrations. The chitosan–QDs film presents good dispersive, uniform, excellent luminescent and good antibacterial properties. Since chitosan used to be a DNA delivery system, the prepared film can be used to study the processes of drug release, and nucleic acid transfection, etc. The highly luminescent L-cysteine functionalized CdTe QDs–chitosan film can be used as a potential tool for biomedical applications and will play a crucial role in biotechnology, biomedicine and molecular biology.

Acknowledgement

The authors are thankful to the University Grants Commission and CSIR, New Delhi for providing financial assistant in the form of major research projects to carry out the work.

References

Aktaş, Y., Yemisci, M., Andrieux, K., Gürsoy, R. N., Alonso, M. J., Fernandez-Megia, E., et al. (2005). Development and brain delivery of chitosan–PEG nanoparticles functionalized with the monoclonal antibody OX26. *Bioconjugate Chemistry*, *6*, 1503–1511.

Bailey, R. E., & Nie, S. (2003). Alloyed semiconductor quantum dots: Tuning the optical properties without chainging the particle size. *Journal of American Chemical Society*, *125*, 7100–7106.

Bao, H., Wang, E., & Dong, S. (2006). One-pot synthesis of CdTe nanocrystal and shape control of luminescent CdTe-cystine nanocomposites. *Small*, *2*, 476–480.

Bruchez, M., Jr., Moronne, M., Gin, P., Weiss, S., & Alivisatos, A. P. (1998). Semiconductor nanocrystals as fluorescent biological labels. *Science*, *281*, 2013–2016.

Chen, H., Lo, B., Hwang, J., Chang, G., Chen, C., Tasi, S., et al. (2004). Colloidal ZnSe, ZnSe/ZnS, and ZnSe/ZnSeS quantum dots synthesized from ZnO. *Journal of Physical Chemistry B*, *108*, 17119–17123.

Chung, Y. C., & Chen, C. Y. (2008). Antibacterial characteristics and activity of acid-soluble chitosan. *Bioresource Technology*, *8*, 2806–2814.

Clark, C. L., Jacobs, M. R. J., & Appelbaum, P. C. (1998). Antipneumococcal activities of levofloxacin and clarithromycin as determined by agar dilution, microdilution, *e*-test, and disk diffusion methodologies. *Journal of Clinical Microbiology*, *36*, 3579–3584.

Demarger-Andre, S., & Domard, A. (1994). Chitosan carboxylic acid salts in solution and in the solid state. *Carbohydrate Polymer*, *23*, 211–219.

Dutta, P. K., Srivastava, R., & Dutta, J. (2013). Functionalized nanoparticles and chitosan-based functional nanomaterials. *Advances in Polymer Science*,. in press

Eugene, K., & Lee, Y. L. (2003). Implantable application of chitin and chitosan. *Biomaterials*, *24*, 2339–2349.

He, Z., Zhu, H., & Zhou, P. (2012). Microwave-assisted aqueous synthesis of highly luminescent carboxymethyl chitosan-coated CdTe/CdS quantum dots as fluorescent probe for live cell imaging. *Journal of Fluorescence*, *22*, 193–199.

Jaiswal, J. K., Mattoussi, H., Mauro, J. M., & Simon, S. M. (2003). Long-term multiple color imaging of live cells using quantum dots bioconjugates. *Nature Biotechnology*, *21*, 47–51.

Jayasree, A., Sasidharan, S., Koyakutty, M., Nair, S., & Menon, D. (2011). Mannosylated chitosan-zinc sulphide nanocrystals as fluorescent bioprobes for targeted cancer imaging. *Carbohydrate Polymers*, *85*, 37–43.

Jessirie, D., Hilton, K., & Amandav, E. (2009). Cadmium sulfide quantum dots/chitosan nanocomposites for latent fingermark detection. *Forensic Science International*, *187*, 97–102.

Jiang, W., Mardyani, S., Fischer, H., & Chan, W. C. W. (2006). Design and characterization of lysine cross-linked mercapto-acid biocompatible quantum dots. *Chemistry of Materials*, *18*, 872–878.

Kumar, S., & Dutta, P. K. (2008). Evaluation of optical photoluminescence properties for cyano based chitosan derivative film. *Asian Chitin Journal*, *4*, 67–74.

Li, Z., Ramay, H. R., Hauch, K. D., Xiao, D., & Zhang, M. (2005). Chitosan–alginate hybrid scaffolds for bone tissue engineering. *Biomaterials*, *26*, 3919–3928.

Li, Y., Jing, L., Qiao, R., & Gao, M. (2011). Aqueous synthesis of CdTe nanocrystals: Progresses and perspectives. *Chemical Communications*, *47*, 9293–9311.

Lin, Y., Zhang, L., Yao, W., Qian, H., Ding, D., Wa, W., et al. (2011). Water-soluble chitosan–quantum dot hybrid nanospheres toward bioimaging and biolabeling. *ACS Applied Material Interfaces*, *3*, 995–1002.

Liong, M., Lu, J., Kovochich, M., Xia, T., Ruehm, S. G., Nol, A. E., et al. (2008). Multifunctional inorganic nanoparticles for imaging, targeting, and drug delivery. *ACS Nano*, *2*, 889–896.

Liu, S., Xue, J., & Ding, W. (2009). Efficient fabrication of transparent antimicrobial poly(vinyl alcohol) thin films. *Journal Nanoparticle Research*, *11*, 553–560.

Luo, Z., Wu, Q., Zhang, M., Li, P., & Ding, Y. (2011). Cooperative antimicrobial activity of CdTe quantum dots with rocephin and fluorescence monitoring for *Escherichia coli*. *Journal of Colloid and Interface Science*, *362*, 100–106.

Mamedov, A. A., Belov, A., Giersig, M., Mamedova, N. N., & Kotov, N. A. (2001). Nanorainbows: Graded semiconductor films from quantum dots. *Journal of American Chemical Society*, *123*, 7738–7739.

Mansur, H. S., Mansur, A. A. P., Curti, E., & Almeida, M. V. D. (2013). functionalized-chitosan/quantum dot nano-hybrids for nanomedicine applications: Towards biolabeling and biosorbing phosphate metabolites. *Journal of Materials Chemistry B*, *1*, 1696–1711.

Maria, T. P., Didier, D., Patrick, C., & d'Angelo, J. (1997). Synthesis of a novel poly(MePEG cyanoacrylate-co-alkyl cyanoacrylate) amphiphilic copolymer for nanoparticle technology. *Macromolecules*, *30*, 846–851.

Medintz, I. L., Uyeda, H. T., Goldman, E. R., & Mattoussi, H. (2005). Quantum dots bioconjugates for imaging, labelling and sensing. *Nature Materials*, *4*, 435–446.

Murray, C. B., Norris, D. J., & Bawendi, M. G. (1993). Synthesis and characterization of nearly monodisperse CdE (E = S, Se, Te) semiconductor nanocrystallites. *Journal of American Chemical Society*, *115*, 8706–8715.

Muzzarelli, R. A. A., & Tanfani, F. (1982). N-(O-carboxybenzyl) chitosan N-carboxymethyl chitosan and dithiocarbamate chitosan: New chelating derivatives of chitosan. *Pure and Applied Chemistry*, *54*, 2141–2150.

Muzzarelli, R. A. A., Boudrant, J., Meyer, D., Manno, N., DeMarchis, M., & Paoletti, M. G. (2012). Current views on fungal chitin/chitosan, human chitinases, food preservation, glucans, pectins and inulin: A tribute to Henri Braconnot, precursor of the carbohydrate polymers science, on the chitin bicentennial. *Carbohydrate Polymers*, *87*, 995–1012.

Muzzarelli, R. A. A., Greco, F., Busilacchi, A., Sollazzo, V., & Gigante, A. (2012). Chitosan, hyaluronan and chondroitin sulfate in tissue engineering for cartilage regeneration: A review. *Carbohydrate Polymers*, *89*, 723–739.

Nath, S., Kaittanis, C., Tinkham, A., & Perez, J. M. (2008). Dextran coated gold nanoparticles for the assessment of antimicrobial susceptibility. *Analytical Chemistry*, *80*, 1033–1038.

Qian, H., Dong, C., Weng, J., & Ren, J. (2006). Facile one-pot synthesis of luminescent, water-soluble, and biocompatible glutathione-coated CdTe nanocrystals. *Small*, *2*, 747–751.

Qu, L. Z., Peng, A., & Peng, X. (2001). Alternative routes toward high quality CdSe nanocrystals. *Nano Letters*, *1*, 333–337.

Rabea, E. I., Badawy, M. E.-T., Stevens, C. V., Smagghe, G., & Steurbaut, W. (2003). Chitosan as antimicrobial agent: Applications and mode of action. *Biomacromolecules*, *4*, 1457–1465.

Rameshkumar, A., Sivasudha, T., Jeyadevi, R., Sangeetha, B., Ananth, D. A., Aseervatham, G. S. B., et al. (2013). In vitro antioxidant and antimicrobial activities of *Merremia emarginata* using thio glycolic acid-capped cadmium telluride quantum dots. *Colloids and Surfaces B: Biointerfaces*, *101*, 74–82.

Ravi Kumar, M. N. V., Muzzarelli, R. A. A., Muzzarelli, C., Sashiwa, H., & Domb, A. J. (2004). Chitosan chemistry and pharmaceutical perspectives. *Chemical Reviews*, *104*, 6017–6084.

Sanpui, P., Pandey, S. B., Chattopadhyay, A., & Ghosh, S. S. (2010). Incorporation of gene therapy vector in chitosan stabilized Mn^{2+}-doped ZnS quantum dots. *Materials Letters*, *64*, 2534–2537.

Singh, J., & Dutta, P. K. (2009). Preparation circular dichroism induced helical conformations and optical property of chitosan acid salt complexes for biomedical applications. *International Journal of Biological Macromolecule*, *45*, 384–392.

Singh, J., Kumar, S., & Dutta, P. K. (2009). Preparation and chiroptical properties of chitosan acid derivatives in dilute solution. *Journal of Polymer Materials*, *26*, 167–176.

Srivastava, R., Tiwari, D. K., & Dutta, P. K. (2011). 4-(Ethoxycarbonyl) phenyl-1-amino-oxobutanoic acid–chitosan complex as a new matrix for silver nanocomposite film: Preparation, characterization and antibacterial activity. *International Journal of Biological Macromolecules*, *49*, 863–870.

Talapin, D. V., Haubold, S., Rogach, A. L., Kornowski, A., Haase, M., & Weller, H. (2001). A novel organometallic synthesis of highly luminescent CdTe nanocrystals. *Journal of Physical Chemistry B*, *105*, 2260–2263.

Yuan, Q., Hein, S., & Misra, R. D. K. (2010). New generation of chitosan-encapsulated ZnO quantum dots loaded with drug: Synthesis, characterization and in vitro drug delivery response. *Acta Biomaterialia*, *6*, 2732–2739.

Zhong, X. H., Han, M. Y., Dong, Z. L., White, T. J., & Knoll, W. (2003). Composition-tunable $Zn_xCd_{1-x}Se$ nanocrystals with high luminescence and stability. *Journal of American Chemical Society*, *125*, 8589–8594.